

Article

Effects of Oxygenated Brackish Water on Pakchoi (*Brassica chinensis* L.) Growth Characteristics Based on a Logistic Crop Growth Model

Yuyang Shan, Yan Sun ^{*}, Wanghai Tao and Lijun Su 

State Key Laboratory of Eco-Hydraulics in Northwest Arid Region of China, Xi'an University of Technology, Xi'an 710048, China; syy031@126.com (Y.S.); xautsoilwater@163.com (W.T.); sljun11@163.com (L.S.)

* Correspondence: sunyan199058@126.com

Abstract: Oxygenated irrigation can improve soil physical and chemical properties and increase vegetable yields. It provides an effective method for safe and efficient utilization of brackish water, but its growth-promoting pathway is unclear. We investigated the effects of brackish water culture at five dissolved oxygen concentrations (9.5 (CK), 12.5, 15.5, 18.5, and 22.5 mg/L) on pakchoi (*Brassica chinensis* L.) growth characteristics by hydroponics experiment, and the logistic model to fit and analyze pakchoi growth characteristics. At a brackish water dissolved oxygen concentration of 18.5 mg/L, nitrogen mass fraction was significantly higher than in a control treatment by 43.4%, and pakchoi effective accumulated temperature increment during vigorous plant height and root length growth was significantly lower than other treatments. The logistic model effectively simulated pakchoi plant height and root length growth, and both theoretical maximum plant height and root length reached their maximum values at 18.5 mg/L dissolved oxygen concentration. Path analysis showed that the maximum net photosynthetic rate and nitrogen mass fraction were the main factors affecting aboveground pakchoi fresh weight. In conclusion, a dissolved oxygen concentration of 18.5 mg/L in brackish water is more appropriate for pakchoi to achieve high yield under brackish water hydroponics conditions. Our results provide guidance for the safe and efficient utilization of brackish water in green and efficient vegetable production.

Keywords: brackish water; dissolved oxygen concentration; pakchoi; logistic model; path analysis



Citation: Shan, Y.; Sun, Y.; Tao, W.; Su, L. Effects of Oxygenated Brackish Water on Pakchoi (*Brassica chinensis* L.) Growth Characteristics Based on a Logistic Crop Growth Model.

Agriculture **2023**, *13*, 1345.
<https://doi.org/10.3390/agriculture13071345>

Academic Editor: Hans Gheyi

Received: 18 May 2023
Revised: 20 June 2023
Accepted: 29 June 2023
Published: 3 July 2023



Copyright: © 2023 by the authors. Licensee MDPI, Basel, Switzerland. This article is an open access article distributed under the terms and conditions of the Creative Commons Attribution (CC BY) license (<https://creativecommons.org/licenses/by/4.0/>).

1. Introduction

Human activities and climate change have made water supply and demand increasingly prominent, especially when demand exceeds supply and restricts sustainable agricultural development [1–3]. Increasingly, more countries and regions are facing severe water shortage challenges [4] and have developed and utilized brackish water to alleviate freshwater shortages [5–7]. Brackish water resources are widely distributed in Northwest China, with huge development potential [8]. However, their long-term use for irrigation will aggravate secondary soil salinization and affect normal crop growth [9,10]. Therefore, how to use brackish water resources for agricultural irrigation in a green and efficient manner plays a vital role in sustainable agricultural production and development.

Oxygenated irrigation is the use of physical or chemical oxygen technology to significantly increase dissolved oxygen content in ordinary water [11,12], thereby increasing irrigation water activity, enhancing its physiological functions, and improving crop water and fertilizer utilization effectiveness. Therefore, combining oxygen technology with brackish water irrigation to develop more efficient aerobic brackish water irrigation technology is highly significant for alleviating water supply and demand contradictions and realizing agricultural water conservation. Presently, commonly used physical oxygenation technologies include micro-nano bubble generators or venturi air jets for hydrogen peroxide solution delivery to crop root zones to achieve oxygenation [13,14]. Among them,

micro-nano bubbles can slowly rise, remain in the water for a long time, dissolve under pressure by themselves, and have a large specific surface area which is beneficial to the mass transfer, adsorption, and chemical reaction of the gas/liquid interface [15].

Oxygen is not only the final electron acceptor of the oxidative phosphorylation pathway in aerobic respiration [16] but also provides most of ATP needed in crop roots through oxidative reaction. As important organs for plant growth, roots not only have many important physiological functions, such as absorption, fixation, storage, synthesis, and reproduction but also profoundly affect plant adaptation to the environment, interspecies competition, and ecological strategies [17,18]. Studies have shown that a suitable rhizosphere oxygen environment can improve yield, quality, and phosphorus utilization efficiency [19] in vegetables, such as lettuce [20] and tomato [21]. However, a root oxygen environment that is too low or too high will also adversely affect vegetable growth. Xu et al. [22] showed that oxygen stress (hypoxia or hyperoxia) accelerates cell senescence and destroys cell membrane permeability. Additionally, active oxygen radicals will be produced under high dissolved oxygen concentrations, and their excessive production may limit vegetable growth and decrease photosynthetic efficiency [23]. Therefore, an appropriate rhizosphere dissolved oxygen concentration is important for vegetable quality and production efficiency.

Crop growth models are the main basis for precision agricultural crop diagnosis and technical measure formulation. They simulate crop growth by applying known or predicted conditions to provide quantitative indicators for decision-making and diagnosis [24]. Crop growth follows certain rules, and organ growth and development ultimately determine crop yields. Currently, the most commonly used crop growth model is the logistic equation, a continuous distribution with greater use value and a common sigmoid function [25–27]. It is suitable for crop organ growth trends where the growth rate is slow-fast-slow. Logistic equations perform well in expressing and quantifying the compensation effect of crop growth characteristics [28–30]. By applying logistic functions, we can improve grain moisture content and daily grain dry weight through simulations [31]. In early applications, the logistic model used time t (time after sowing or time after emergence) as an independent variable to simulate and analyze temporal crop growth and crop dry matter accumulation changes after emergence in an S-shaped curve [32]. However, due to different climate conditions and crop growth times in different regions, the crop growth stage expressed by growth time alone will produce larger deviations [33]. Since the heat required by crops to complete a certain growth stage is constant, we used effective accumulated temperature instead of time to simulate crop growth and development [34,35].

Overall, oxygenated irrigation has been widely studied in vegetables, while its impact in combination with brackish water on vegetable growth characteristics has been rarely reported. Pakchoi is one of the most popular vegetable crops because of its short growth period, easy planting, and high nutritional value [36,37]. Therefore, we explored the effect of brackish water culture with different dissolved oxygen concentrations on pakchoi growth characteristics. Furthermore, based on effective accumulated temperature, we used the logistic model to study pakchoi dynamic growth changes. Concurrently, the suitable dissolved oxygen concentration under brackish water culture was identified to provide a feasible method for safe and efficient brackish water utilization.

2. Materials and Methods

2.1. Experimental Design

The experiment was conducted hydroponically in an artificial climate greenhouse, with a temperature of 25 °C, a humidity of 40%, and a natural light source. Plump pakchoi seeds (Four Seasons King Shanghai Qing) were selected and placed in a culture medium for cultivation. When seedlings were 3–5 cm tall, one for each growth condition was transplanted into a plastic bucket (base area 20 cm² and height 15 cm). A hydroponic nutrient solution was prepared, composed of Hoagland nutrient solution (Table 1) and sodium chloride (content \geq 99.5%, pure AR for analysis), with salinity set to 3 g/L. The

plastic bucket was wrapped with tin foil to provide a dark environment for pakchoi root growth. After the pakchoi were transplanted, they were cultivated with a 1/4 concentration nutrient solution for 6 days, a 1/2 concentration nutrient solution for 6 d, and then a full concentration nutrient solution until the pakchoi was harvested. The culture medium was replaced every 48 h. Before transplanting and each nutrient solution change, the brackish water was treated with different oxygenation levels: Treatment 1 was solely brackish water without oxygenated treatment (dissolved oxygen concentration of 9.5 mg/L), and the dissolved oxygen concentrations of the other four oxygenation treatments were 12.5, 15.5, 18.5, and 22.5 mg/L, respectively. Six replicates were established for each oxygenated treatment, and the non-oxygenated treatment was used as the control (CK). A micro-nano bubble rapid generation device was used for oxygenation, and an HQ40 portable dissolved oxygen meter was used to monitor brackish water dissolved oxygen concentration changes during oxygenation.

Table 1. Formula of Hoagland nutrient solution.

Macronutrients		Micronutrients		Formula of FeEDTA Solution	
Salts	Concentration/(g·L ⁻¹)	Salts	Concentration/(mg·L ⁻¹)	Category	Concentration in FeEDTA Solution/(g·L ⁻¹)
Ca(NO ₃) ₂ ·4H ₂ O	1.18	H ₃ BO ₃	2.86	FeSO ₄ ·7H ₂ O	5.56
KNO ₃	0.51	MnCl ₂ ·4H ₂ O	1.81		
MgSO ₄ ·7H ₂ O	0.49	ZnSO ₄ ·7H ₂ O	0.22	C ₁₀ H ₁₄ N ₂ Na ₂ O ₈ ·2H ₂ O (EDTA-Na ₂)	7.46
KH ₂ PO ₄	0.14	CuSO ₄ ·5H ₂ O	0.08		
		H ₂ MoO ₄ ·H ₂ O/Na ₂ MoO ₄ ·2H ₂ O	0.02/0.03		

Note: 2 mL of FeEDTA solution was added to each liter of culture solution.

2.2. Measurement Index and Method

The nutrient solution was collected every 2 days during pakchoi growth, and nitrate nitrogen content was measured with an ultraviolet spectrophotometer. Pakchoi leaf nitrogen mass fractions were determined with an elemental analyzer (UNICUBE, Elementar Trading (Shanghai) Co., Ltd., Shanghai, China). Pakchoi plant height and taproot root length were measured with a steel ruler every 2 to 4 days. At the mature stage (50 days after transplanting), the fresh weight of the aboveground plant parts of each treatment was weighed.

2.3. The Logistic Model of Crop Growth

The specific formula [38] of the logistic model of crop growth is expressed as:

$$H = \frac{H_m}{(1 + e^{a_1 + b_1 GDD})} \quad (1)$$

$$M = \frac{M_m}{(1 + e^{a_2 + b_2 GDD})} \quad (2)$$

where H is plant height, cm; M is root length, cm; H_m is the theoretical upper limit of plant reproduction, cm; M_m is the theoretical upper limit of root reproduction, cm; GDD is the effective accumulated temperature after sowing; a_1 , b_1 are undetermined coefficients.

In this experiment, pakchoi seeds were first grown into seedlings and then transferred into nutrient solution to continue growth hydroponically. Therefore, based on the original logistic equation and initial plant height and root length at the beginning of hydroponics, the modified equation is as follows:

$$H = \frac{H_m}{(1 + e^{a_1 + b_1 GDD})} + h \quad (3)$$

$$M = \frac{M_m}{(1 + e^{a_2 + b_2 GDD})} + m \quad (4)$$

where H is plant height, cm; M is root length, cm; H_m is the theoretical plant height in reproduction, cm; M_m is the theoretical root length in reproduction, cm; GDD is effective after sowing accumulated temperature; a_1, b_1, a_2, b_2 are undetermined coefficients; h is initial plant height when hydroponics began, m is initial root length when hydroponics began.

Crops can only absorb energy and continue to grow within a suitable temperature range. High or low temperatures can inhibit growth and even cause damage to crops. Effective accumulated temperature (GDD) refers to the sum of the temperature difference between the daily average temperature after crop sowing and the lower limit of biological temperature suitable for crop growth [39]. Its expression is:

$$GDD = \sum_{i=1}^n (T_{avg_i} - T_{base_i}) \quad (5)$$

In the formula, T_{avg_i} is the average daily temperature (this experiment was carried out in an intelligent artificial climate greenhouse, which is a constant temperature of 25 °C), and T_{base_i} is the biological lower limit temperature (the pakchoi biological lower limit temperature is 4 °C).

2.4. Correlation Analysis and Path Analysis

The photosynthetic characteristics parameters and yield data of pakchoi were obtained from Sun et al. [40]. The results analysis and discussion of this manuscript did not directly use and describe these published data but further used the path analysis method to deeply discuss the relationship between the photosynthetic characteristics parameters and yield of pakchoi and the data of plant height, root length, and nitrogen mass fraction in this manuscript, so as to further explore and analyze the impact of various factors on the pakchoi yield under brackish water culture with different dissolved oxygen concentrations. In addition, the growth conditions of pakchoi in the published paper were consistent with the present manuscript.

All measured data were recorded in Excel 2019 and examined with analysis of variance (ANOVA) using IBM SPSS 22.0 software (IBM Corp., Armonk, NY, USA). Correlation analysis and path analysis were performed using Python 3.8. Significant differences ($p < 0.05$) between means were identified using the least significant difference (LSD) test. Figures were drawn using Origin 2021 software.

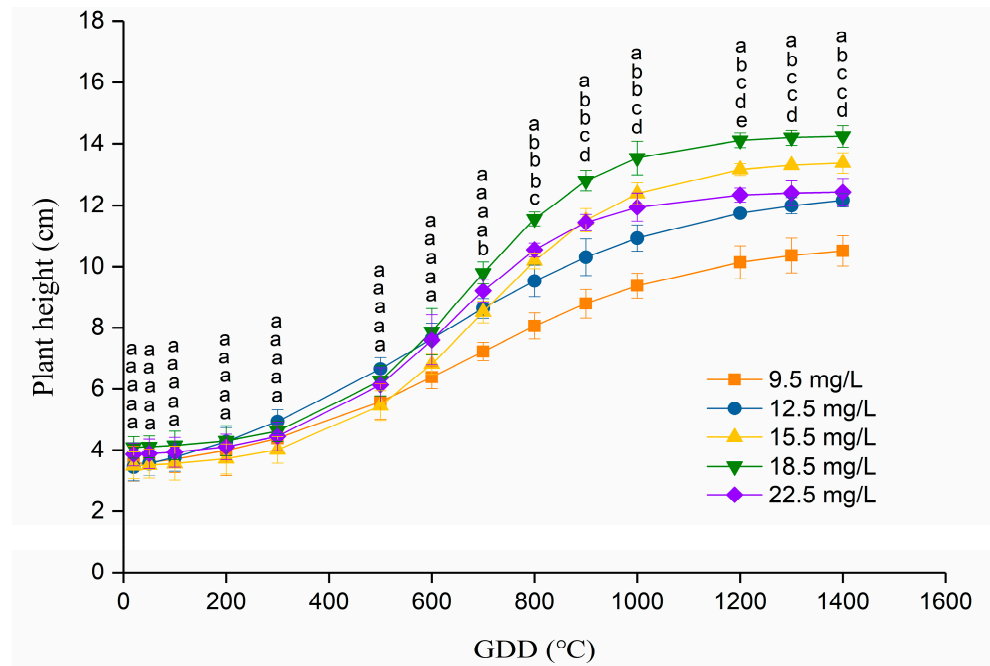
3. Results

3.1. The Relationship between Effective Accumulated Temperature and Plant Height and Root Length

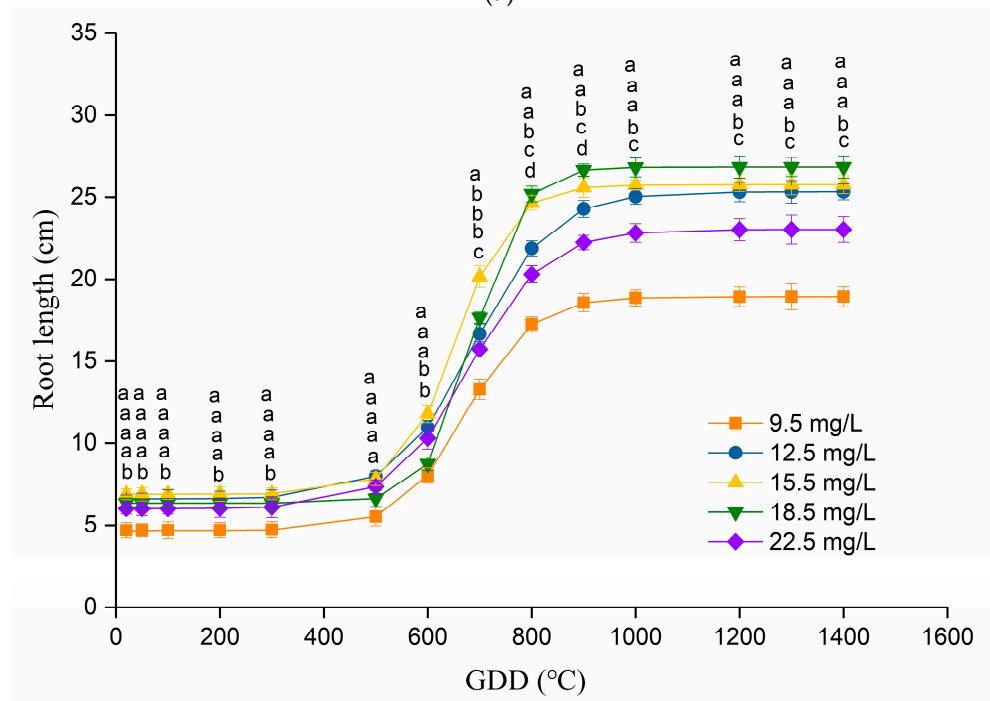
Different oxygenation treatments of brackish water could significantly promote the growth characteristics (plant height and root length) of pakchoi. For plant height, when the GDD was greater than 700 °C, there was a significant difference ($p < 0.05$) under different dissolved oxygen concentrations in brackish water compared with that non-oxygenated treatment (9.5 mg/L). For root length, when the GDD was greater than 600 °C, brackish water at different dissolved oxygen concentrations had significant differences ($p < 0.05$) compared with that non-oxygenated treatment (9.5 mg/L). Especially at the late growth stage of pakchoi, the difference between 9.5 mg/L treatment and 18.5 mg/L treatment was more significant.

Pakchoi plant height growth was in accordance with the logistic model (Figure 1a). The fitting curves of the five treatment groups' coefficients of determination were >0.99 , and the fitting degree was good (Table 2). With increasing brackish water oxygenation level, the theoretical upper limit of pakchoi plant height initially increased and then decreased. When brackish water dissolved oxygen concentration increased to 18.5 mg/L, the theoretical upper limit of pakchoi plant height reached a maximum, but when it increased to 22.5 mg/L, the theoretical upper limit of pakchoi plant height decreased. Among them, the theoretical upper limit of pakchoi plant height at 12.5, 15.5, 18.5, and 22.5 mg/L oxy-

gen concentration increased by 31.46, 31.63, 34.94, and 13.94%, respectively, compared to no oxygen.



(a)



(b)

Figure 1. The relationship between the effective accumulated temperature (*GDD*) and the theoretical upper limit of plant height (a) and root length (b) of pakchoi cultured in brackish water with different dissolved oxygen concentrations. The different lowercase letters at the same *GDD* (effective accumulated temperature) indicate significant differences among different treatments ($p < 0.05$).

Table 2. The characteristic values of curve fitting of pakchoi cultured in brackish water with different dissolved oxygen concentrations.

Index	Dissolved Oxygen Concentration/(mg/L)	$H_m(M_m)/\text{cm}$	$H_m'(M_m')/\text{cm}$	$a_1(a_2)$	$b_1(b_2)$	R^2	$h(m)/\text{cm}$
Plant height	9.5	7.617	10.782	3.014	−0.0045	0.997	3.165
	12.5	10.013	12.543	2.355	−0.004	0.994	2.529
	15.5	10.026	13.440	4.869	−0.007	0.990	3.414
	18.5	10.278	14.291	5.068	−0.0076	0.992	4.013
	22.5	8.679	12.455	4.736	−0.0075	0.984	3.776
Root length	9.5	14.236	18.929	10.779	−0.016	0.994	4.693
	12.5	18.717	25.326	9.231	−0.0134	0.992	6.609
	15.5	18.859	25.758	12.509	−0.0191	0.994	6.899
	18.5	20.492	26.838	15.402	−0.0223	0.991	6.346
	22.5	17.015	23.028	9.305	−0.0137	0.995	6.013

H_m is the theoretical upper limit of plant height of pakchoi; M_m is the theoretical upper limit of root length of pakchoi; H_m' is the theoretical upper limit of plant height of pakchoi after modification; M_m' is the theoretical upper limit of root length of pakchoi after modification; a_1, b_1, a_2, b_2 are undetermined coefficients; h is the initial plant height of pakchoi before transplanting; m is the initial root length of pakchoi before transplanting.

Root length fitting results also conformed to the logistic model (Figure 1b), fitting curves R^2 of the five treatments were all >0.99 , and curve fitting accuracy was high (Table 2). When the effective accumulated temperature GDD was $650\text{ }^\circ\text{C}$, the pakchoi root length growth rate was the highest, but when GDD was $>650\text{ }^\circ\text{C}$, it gradually decreased. When the effective accumulated temperature GDD was $>800\text{ }^\circ\text{C}$, the root length growth rate approached zero. As brackish water dissolved oxygen concentration increased from 9.5 to 18.5 mg/L , the theoretical upper limit of pakchoi root length showed an increasing trend. However, when it increased to 22.5 mg/L , the theoretical upper limit of pakchoi root length was lower than at 18.5 mg/L . Among them, compared with the unoxygenated treatment, the theoretical upper limit of pakchoi root length increased by 31.48 , 32.47 , 43.94 , and 17.02% , respectively, under oxygen concentrations of 12.5 , 15.5 , 18.5 , and 22.5 mg/L .

3.2. Pakchoi Growth Dynamics

The derivation of Equations (3) and (4) was successively obtained. When the first derivative is the largest (the second derivative is zero), that is, $GDD = GDD_0 = -a_1/b_1$, the growth rate is greatest. After this point, the growth rate decreases and then gradually approaches zero. Since pakchoi plant height and root length conformed with the logistic model, the two model inflection points, i.e., the extreme point of the second derivative (the third derivative is zero), can be used to obtain the most vigorous pakchoi growth stage. Two characteristic points are obtained: $GDD_1 = \frac{\ln(2+\sqrt{3})-a_1}{b_1}$, $GDD_2 = \frac{\ln(2-\sqrt{3})-a_1}{b_1}$. The difference between GDD_1 and GDD_2 is ΔGDD , which is the pakchoi effective accumulated temperature increment during vigorous plant height and root length growth (Table 3).

ΔGDD is the vigorous pakchoi plant height or root length growth period and can reflect the increase in effective accumulated temperature required by the crop in the rapid growth stage. Therefore, when dissolved oxygen concentration was 18.5 and 22.5 mg/L , plant height ΔGDD was significantly lower than in other dissolved oxygen treatments (Table 4). Especially, the root length ΔGDD under the treatments with a dissolved oxygen concentration of 18.5 mg/L was significantly lower than other dissolved oxygen treatments. Simultaneously, plant height and root length under 18.5 mg/L dissolved oxygen concentration were significantly higher than in other treatments. This indicated that the increase in effective accumulated temperature required to maintain pakchoi rapid growth under this treatment was the lowest, but growth efficiency was the highest.

3.3. Cumulative Consumption of Nitrate Nitrogen under Different Dissolved Oxygen Concentration

Nitrate nitrogen cumulative consumption generally showed an increasing trend (Figure 2) and increased significantly between 11 and 27 days after transplanting but decreased 21 days after transplanting. The cumulative rate of nitrate nitrogen consumption 39 days after transplanting was basically zero. Pakchoi cumulative nitrate nitrogen consumption at a dissolved oxygen concentration of 18.5 mg/L was significantly lower than other treatments, especially 15 days after the transplanting of pakchoi seedlings ($p < 0.05$, Table 4, Figure 2). However, the nitrogen mass fraction under a dissolved oxygen concentration of 18.5 mg/L was significantly higher than the other treatments ($p < 0.05$, Table 4), which significantly increased by 18.9 , 9.5 , 6.1 , and 8.5% in the 9.5 , 12.5 , 15.5 , and 22.5 mg/L treatments, respectively. This indicated that pakchoi, at the dissolved oxygen concentration of 18.5 mg/L had the highest nitrate nitrogen utilization efficiency.

Table 3. Characteristic values of effective accumulated temperature of plant height and root length under different dissolved oxygen concentrations.

Index	Dissolved Oxygen Concentration/(mg/L)	$GDD_0/^\circ\text{C}$	$GDD_1/^\circ\text{C}$	$GDD_2/^\circ\text{C}$	$\Delta GDD/^\circ\text{C}$
Plant height	9.5	669.778	377.120	962.435	585.315
	12.5	588.750	259.511	917.989	658.479
	15.5	695.571	507.435	883.708	376.274
	18.5	666.842	493.558	840.126	346.568
	22.5	631.467	455.872	807.061	351.189
Root length	9.5	673.688	591.378	673.688	164.620
	12.5	688.881	590.600	787.161	196.561
	15.5	654.921	585.971	723.872	137.901
	18.5	690.673	631.616	749.729	118.113
	22.5	679.197	583.069	775.325	192.257

GDD_0 is the effective accumulated temperature when the growth rate of plant height and root length is the fastest; GDD_1 and GDD_2 are the inflection points of the logistic model; $\Delta GDD = GDD_2 - GDD_1$, which is the effective accumulated temperature increment of pakchoi during vigorous growth of plant height and root length.

Table 4. The relationship between the growth characteristics of pakchoi and the dissolved oxygen concentration.

Dissolved Oxygen Concentration/(mg/L)	Cumulative Consumption of Nitrate Nitrogen/(mg/L)	Nitrogen Mass Fraction	Plant Height $\Delta GDD/^\circ\text{C}$	Root Length $\Delta GDD/^\circ\text{C}$
9.5	2594.70 \pm 57.32 ^b	3.65 \pm 0.11 ^c	585.32 \pm 9.11 ^b	164.62 \pm 10.83 ^b
12.5	2775.84 \pm 20.91 ^a	3.96 \pm 0.10 ^b	658.48 \pm 11.08 ^a	196.56 \pm 3.90 ^a
15.5	2849.53 \pm 127.05 ^a	4.09 \pm 0.15 ^b	376.27 \pm 9.29 ^c	137.90 \pm 10.75 ^c
18.5	1856.56 \pm 40.32 ^c	4.34 \pm 0.11 ^a	346.57 \pm 21.04 ^d	118.11 \pm 5.33 ^d
22.5	2815.78 \pm 56.24 ^a	4.00 \pm 0.04 ^b	351.19 \pm 12.301 ^d	192.26 \pm 16.64 ^a

ΔGDD is the effective accumulated temperature increment of pakchoi during vigorous growth of plant height and root length. The different lowercase letters in a column indicate significant differences among different treatments ($p < 0.05$).

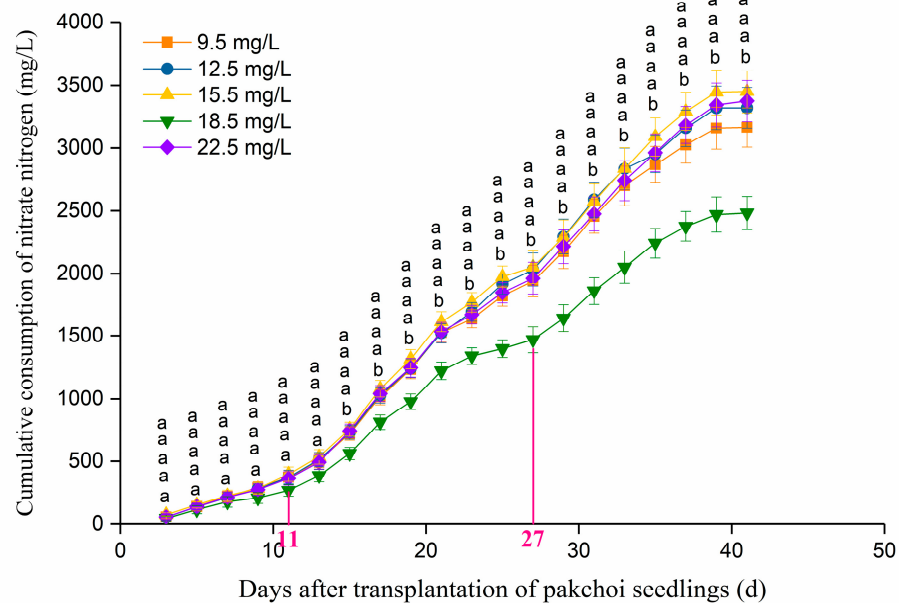


Figure 2. Cumulative consumption of nitrate nitrogen in pakchoi cultured in brackish water with different dissolved oxygen concentrations. The different lowercase letters at the same days after transplantation of pakchoi seedlings indicate significant differences among different treatments ($p < 0.05$).

3.4. Correlation Analysis between Pakchoi Fresh Weight and Various Factors under Different Dissolved Oxygen Concentrations

Fresh weight was significantly and positively correlated with the maximum net photosynthetic rate and nitrogen mass fraction ($p < 0.01$, Table 5), and was significantly and negatively correlated with root length Δ GDD ($p < 0.05$, Table 5). There was a significant positive correlation between the maximum net photosynthetic rate and nitrogen mass fraction ($p < 0.05$, Table 5), and between plant height and root length ($p < 0.05$, Table 5). Therefore, nitrogen content and the maximum net photosynthetic rate were the two most important factors affecting pakchoi fresh weight.

The path coefficient can reflect direct and indirect effects in the correlation coefficient, so the internal action mechanism among the variables can be determined. In this study, we investigated the path analysis between pakchoi fresh weight and various factors (Table 6) and showed that the nitrogen mass fraction direct path coefficient was the largest and the main factor directly affecting fresh weight. The direct path coefficient was positive, and the indirect effect was negative. However, the absolute value of the direct path coefficient was significantly greater than the indirect path coefficient, so the nitrogen mass fraction overall promoted fresh weight. Additionally, the direct and total indirect path coefficients of the maximum net photosynthetic rate on fresh weight were both positive, which had a superimposed positive effect on fresh weight. Therefore, the correlation coefficient between the maximum net photosynthetic rate and fresh weight was the largest, and their correlation was the strongest. Among them, the total indirect effect of the maximum net photosynthetic rate on fresh weight was significantly greater than the direct effect (Table 6), indicating that the maximum net photosynthetic rate mainly affected pakchoi aboveground fresh weight through indirect positive effects. Meanwhile, the indirect path coefficient of the maximum net photosynthetic rate to fresh weight through nitrogen mass fraction was larger (2.272), indicating that the maximum net photosynthetic rate mainly promoted fresh weight through the nitrogen mass fraction. Moreover, the coefficient of determination represents the relative degree of determination of each influencing factor to the predictor. In this study, the nitrogen mass fraction on the fresh weight coefficient of determination was 5.954, and the degree of determination was the largest (Table 7).

Table 5. Correlation coefficients between different growth characteristics of pakchoi.

	Yield	DOC	AqE	LCP	LSP	R _d	P _{nmax}	Plant Height	Root Length	NMF	Plant Height ΔGDD	Root Length ΔGDD
Yield	1.000	0.292	0.760	−0.203	0.647	0.745	0.989 **	0.585	0.325	0.973 **	−0.63	−0.896 *
DOC		1.000	−0.248	0.687	0.657	0.555	0.169	0.567	0.442	0.426	−0.821	−0.057
AqE			1.000	−0.647	0.011	0.368	0.840	0.271	0.144	0.620	0.018	−0.662
LCP				1.000	0.479	0.440	−0.289	0.557	0.628	−0.128	−0.507	0.136
LSP					1.000	0.776	0.550	0.650	0.424	0.742	−0.961 **	−0.679
R _d						1.000	0.715	0.968 **	0.842	0.705	−0.741	−0.754
P _{nmax}							1.000	0.563	0.329	0.93 *	−0.516	−0.031
Plant height								1.000	0.947 *	0.526	−0.633	−0.593
Root length									1.000	0.232	−0.397	−0.383
NMF										1.000	−0.752	−0.836
Plant height ΔGDD											1.000	0.544
Root length ΔGDD												1.000

DOC, dissolved oxygen concentration; AqE, apparent quantum efficiency; LCP, light compensation point; LSP, light saturation point; R_d, dark respiratory rate; P_{nmax}, maximum net photosynthetic rate; NMF, nitrogen mass fraction. ΔGDD is the effective accumulated temperature increment of pakchoi during vigorous growth of plant height and root length. * $p < 0.05$, ** $p < 0.01$. Data on photosynthetic characteristic parameters and yield of pakchoi were from Sun et al. [40].

Table 6. Path coefficient between yield and other growth characteristics of pakchoi.

Independent Variable	Correlation Coefficient	Direct Path Coefficient	Indirect Path Coefficient											
			Total Indirect Effect	DOC	AqE	LCP	LSP	R _d	P _{nmax}	Plant Height	Root Length	NMF	Plant Height ΔGDD	Root Length ΔGDD
DOC	0.292	−1.220	1.509		−0.043	1.078	−0.268	0.642	0.033	0.252	−0.566	1.039	−0.594	−0.064
AqE	0.760	0.170	0.585	0.302		−1.015	−0.005	0.425	0.162	0.120	−0.184	1.514	0.013	−0.747
LCP	−0.203	−1.772	1.570	−0.836	−0.113		−0.195	0.509	−0.056	0.247	−0.804	−0.312	−0.366	0.154
LSP	0.647	−0.410	1.055	−0.800	0.002	0.752		0.897	0.106	0.289	−0.542	1.812	−0.695	−0.767
R _d	0.745	−0.411	1.160	−0.676	0.064	0.690	−0.316		0.138	0.431	−1.077	1.722	−0.536	−0.851
P _{nmax}	0.989	0.190	0.796	−0.206	0.147	−0.454	0.827	0.109		0.251	−0.419	2.272	−0.373	−1.023
Plant height	0.585	0.440	0.140	−0.690	0.047	0.874	−0.265	1.119	0.179		−1.211	1.284	−0.457	−0.669
Root length	0.325	−1.280	1.605	−0.538	0.025	0.986	−0.173	0.973	0.063	0.421		0.567	−0.287	−0.432
NMF	0.973	2.440	−1.469	−0.518	0.108	−0.200	−0.302	0.815	0.179	0.234	−0.297		−0.544	−0.944
Plant height ΔGDD	−0.630	0.720	−1.353	1.000	0.003	−0.795	0.392	−0.857	−0.099	−0.281	0.508	−1.837		0.614
Root length ΔGDD	−0.896	1.130	−2.025	0.069	−0.116	0.214	0.277	−0.872	−0.175	−0.264	0.490	−2.042	0.393	

DOC, dissolved oxygen concentration; AqE, apparent quantum efficiency; LCP, light compensation point; LSP, light saturation point; R_d, dark respiratory rate; P_{nmax}, maximum net photosynthetic rate; NMF, nitrogen mass fraction. ΔGDD is the effective accumulated temperature increment of pakchoi during vigorous growth of plant height and root length. Data on photosynthetic characteristic parameters and yield of pakchoi were from Sun et al. [40].

Table 7. Coefficient of determination between yield and other growth characteristics of pakchoi.

Independent Variable	Direct Decision	Joint Decision										
		DOC	AqE	LCP	LSP	R _d	P _{nmax}	Plant Height	Root Length	NMF	Plant Height ΔGDD	
DOC	1.488											
AqE	0.029	0.103										
LCP	2.465	2.631	0.345									
LSP	0.168	0.657	0.002	0.617								
R _d	1.346	1.571	0.145	1.602	0.738							
P _{nmax}	0.036	0.078	0.054	0.173	0.086	0.315						
Plant height	0.194	0.609	0.041	0.769	0.235	0.988	0.094					
Root length	1.638	1.380	0.063	2.525	0.445	2.500	0.159	1.066				
NMF	5.954	3.815	0.262	3.952	1.297	5.451	0.562	2.120	5.681			
Plant height ΔGDD	0.518	1.443	0.004	1.145	0.568	1.238	0.141	0.401	0.732	2.351		
Root length ΔGDD	1.277	0.157	0.254	0.484	0.630	1.977	0.389	0.590	1.108	3.160		0.885

DOC, dissolved oxygen concentration; AqE, apparent quantum efficiency; LCP, light compensation point; LSP, light saturation point; R_d, dark respiratory rate; P_{nmax}, maximum net photosynthetic rate; NMF, nitrogen mass fraction. ΔGDD is the effective accumulated temperature increment of pakchoi during vigorous growth of plant height and root length. Data of photosynthetic characteristic parameters and yield of pakchoi were from Sun et al. [40].

4. Discussion

4.1. Oxygenation Effects on Pakchoi Growth Characteristics

Oxygen is the reducing power necessary for normal physiological metabolism, crop growth, and development and constitutes the core of the whole-life metabolic crop process [41,42]. However, adverse stress or an inappropriate oxygen environment can easily lead to crop oxygen stress. When crops grow under adverse conditions (such as salt stress), reactive oxygen species production will be stimulated, and their levels will subject crops to different degrees of oxygen stress [43,44]. Under non-oxygenated conditions, a certain degree of salt stress in crops can make the production and elimination of reactive oxygen species relatively stable [45]. This is because salt stress can stimulate reactive oxygen species production in crops, which will lead to oxygen stress, and the reactive oxygen species can increase crop tolerance to oxygen stress by redox modification of target molecules to ensure normal crop growth and development [46]. For oxygenation, the oxygenation method we adopted was achieved by changing the number of micro-nanobubbles in the nutrient solution and then setting different dissolved oxygen concentrations. Studies have shown that micro-nanobubbles will constantly rupture with time, and hydroxyl radicals (a kind of reactive oxygen species) will also be generated during micro-nanobubble bursting [47]. When crops are exposed to oxygen stress (hypoxia or hyperoxia), the balance between active oxygen production and the scavenging system will be broken, meaning that hydroxyl free radicals with high redox potential and strong oxidation cannot be destroyed and removed in time to prevent crop metabolic disorders, thus affecting normal growth and development [48]. However, under appropriate dissolved oxygen concentrations, the antioxidant system can maintain the balance between the production and elimination of reactive oxygen species, thus protecting plant cells from hydroxyl radical harm [49].

In this study, there was a significant difference in pakchoi nitrogen mass fraction under oxygenation and non-oxygenation treatments ($p < 0.05$, Table 4). Under low (12.5 and 15.5 mg/L) or high oxygen (22.5 mg/L) stress, the salt and oxygen stress coupling effect would inhibit nitrogen accumulation in pakchoi leaves. When active oxygen surges significantly over a short time, the balance between active oxygen generation and elimination will be broken, resulting in hydroxyl free radicals (one active oxygen) with high redox potential and strong oxidation generated and unable to be removed by some antioxidant enzymes in time, causing crop metabolic disorders and thus affecting nutrient absorption and utilization [50]. When crops are subjected to high oxygen stress, the photosynthetic rate can be reduced, leading to a decrease in CO₂ availability, thereby hindering the fixation of carbon and nitrogen by crops [51]. When dissolved oxygen concentration was 18.5 mg/L, accumulated nitrate nitrogen consumption of pakchoi leaves was the lowest, and nitrogen mass fraction was the highest, indicating that pakchoi utilization efficiency of nitrate nitrogen under this dissolved oxygen concentration was the highest (Table 4). Moreover, at this dissolved oxygen concentration, the pakchoi antioxidant system produced could not only timely remove the reactive oxygen species generated by the coupling of salt stress and micro-nano bubble cracking, but also the adequate oxygen supply environment could better promote pakchoi nitrogen absorption and utilization. Additionally, studies have shown that there is a significant correlation between crop photosynthetic capacity and nitrogen use efficiency [52–54]. Higher nitrogen use efficiency can significantly improve leaf chlorophyll fluorescence characteristics, increase leaf net photosynthetic rate, and ultimately promote crop yield. This is consistent with our path analysis results. Leaf nitrogen mass fraction was the decisive factor affecting the maximum net photosynthetic rate, which, in turn, significantly affected pakchoi yield (Tables 4–6).

Crops transmit signals to the aboveground canopy through roots and then transport and store growth substances, such as water and nutrients, in crop aboveground parts [55]. Plant height is a key measure of crop aboveground growth, which can effectively reflect plant development and lay a foundation for improving dry matter accumulation and optimizing yield [56]. When the dissolved oxygen concentration was 18.5 mg/L, the pakchoi antioxidant system and dissolved oxygen growth promotion effect in the external

environment made the theoretical upper limit of plant height and root length higher than other treatments (Figure 2), which also lays a certain foundation for obtaining high pakchoi yield under this dissolved oxygen concentration. Additionally, plant height and root length ΔGDD , respectively, represent the vigorous plant height and root length growth period, i.e., the effective accumulated temperature pakchoi growth amount to maintain rapid growth. When the dissolved oxygen concentration was 12.5 mg/L, plant height and root length ΔGDD , respectively, were significantly greater than other treatments ($p < 0.05$, Table 4). Because pakchoi may be affected by excessive hydroxyl radicals caused by salt stress and external micro-nano bubble rupture at this dissolved oxygen concentration, reducing the damage by higher effective accumulated temperature growth is required to maintain normal pakchoi growth. When the dissolved oxygen concentration was 18.5 mg/L, plant height and root length ΔGDD were significantly lower than other treatments ($p < 0.05$, Table 4), indicating that pakchoi may be less harmed by the hydroxyl radicals stimulated by salt stress and external micro-nano bubble rupture. Promoting pakchoi growth by dissolved oxygen may occupy the dominant position, making the effective accumulated temperature increase required by pakchoi in its vigorous growth period lower, the growth rate faster, and the net photosynthetic rate higher. Therefore, when the dissolved oxygen concentration was 18.5 mg/L, a lower effective accumulated temperature was required to obtain a higher pakchoi yield.

4.2. Establishment of Multiple Regression Equation Based on Key Factors

In multiple linear regression analysis, if variables are highly correlated (i.e., there is multiple collinearity), the regression model parameter estimates will be unstable. The simplest and most direct solution to this is to reduce the number of variables. Path analysis can deal with more complex variable relationships, separate the key factors from more original variables, and thus reflect the important role of key independent variables in regression equations.

According to path analysis results, we concluded that the dissolved oxygen concentration in different nutrient solutions affects pakchoi leaf nitrogen mass fractions and that they had the greatest impact on the maximum net photosynthetic rate, which was positively correlated with yield (Table 5). Therefore, pakchoi aboveground fresh weight (y) was fitted by a linear equation with dissolved oxygen concentration (x_1) and nitrogen mass fraction (x_2):

$$y = 7.069 - 0.1508 x_1 + 4.79 x_2 \quad (6)$$

$$R^2 = 0.96$$

From Equation (6), the equation fitting degree was good ($R^2 = 0.9651$, Figure 3). The linear equation fitted by the scatter was $y = x - 0.0003$, almost coinciding with the linear equation $y = x$, indicating that the aboveground pakchoi fresh weight value predicted by the established regression equation was close to the measured value and that the multivariate regression equation prediction accuracy was high.

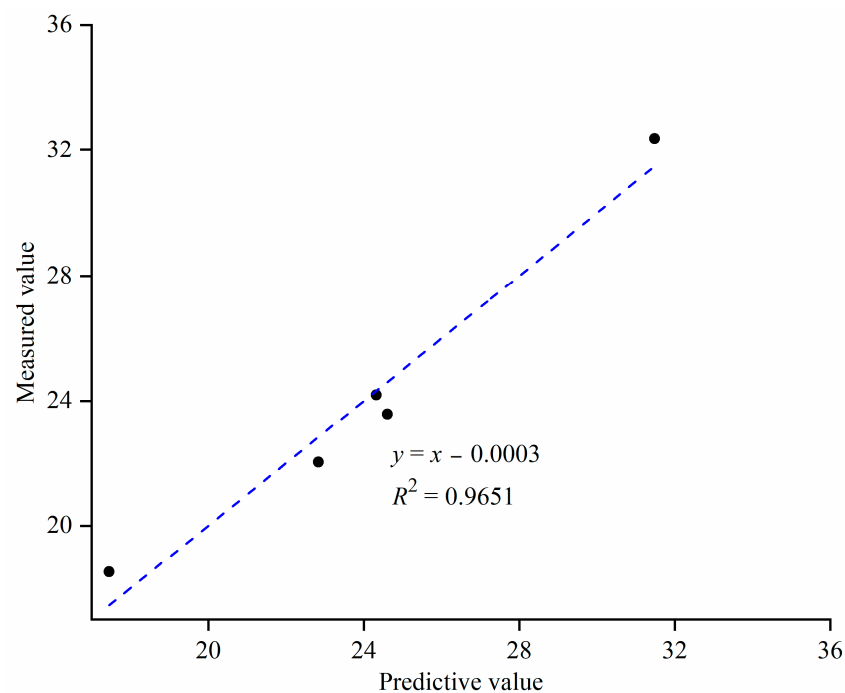


Figure 3. Scatter distribution for predictive value and measured value of fresh weight of aboveground part of pakchoi.

5. Conclusions

In brackish water culture with different dissolved oxygen concentrations, pakchoi plant height and root length growth were well described by the logistic curve ($R^2 > 0.99$), and the fitting degree was high. The most suitable brackish water dissolved oxygen concentration for hydroponic pakchoi was 18.5 mg/L, and at this oxygen concentration pakchoi had higher nitrate nitrogen absorption and utilization efficiency, faster growth rate, and higher leaf photosynthesis efficiency, thus obtaining higher pakchoi yield. The regression equation of pakchoi aboveground fresh weight using dissolved oxygen concentration and nitrogen mass fraction of brackish water confirmed that they were the key predictors with high prediction accuracy.

Author Contributions: Methodology, W.T. and L.S.; Project administration, Y.S. (Yan Sun) and W.T.; Visualization, W.T. and L.S.; Writing—original draft, Y.S. (Yuyang Shan); Writing—review & editing, Y.S. (Yan Sun). All authors have read and agreed to the published version of the manuscript.

Funding: The present research was funded by the National Natural Science Foundation of China (41830754, 52109064), the Yulin City Science and Technology Plan Project (CXY-2021-136), the Major Science and Technology projects of the XPCC (2021AA003-2).

Institutional Review Board Statement: Not applicable.

Data Availability Statement: The corresponding author can provide the data used in this work upon request.

Conflicts of Interest: The authors declare no conflict of interest.

References

1. Mu, L.; Liu, Y.H.; Chen, S.J. Alleviating water scarcity and poverty through water rights trading pilot policy: A quasi-natural experiment based approach. *Sci. Total Environ.* **2022**, *823*, 153318. [[CrossRef](#)] [[PubMed](#)]
2. Lee, J.; Shin, H. Agricultural reservoir operation strategy considering climate and policy changes. *Sustainability* **2022**, *14*, 9014. [[CrossRef](#)]
3. Garcia-Tejero, I.F.; Duran-Zuazo, V.H. Plant water use efficiency for a sustainable agricultural development. *Agronomy* **2022**, *12*, 1806. [[CrossRef](#)]

4. Ma, W.; Meng, L.; Wei, F. Spatiotemporal variations of agricultural water footprint and socioeconomic matching evaluation from the perspective of ecological function zone. *Agric. Water Manag.* **2021**, *249*, 106803. [[CrossRef](#)]
5. Yuan, C.F.; Feng, S.Y.; Huo, Z.L.; Ji, Q.Y. Simulation of saline water irrigation for seed maize in arid northwest China based on SWAP model. *Sustainability* **2019**, *11*, 4264. [[CrossRef](#)]
6. El-Fakharany, Z.M.; Salem, M.G. Mitigating climate change impacts on irrigation water shortage using brackish groundwater and solar energy. *Energy Rep.* **2021**, *7*, 608–621. [[CrossRef](#)]
7. Hamdan, H.; Saidy, M.; Alameddine, I.; Al-Hindi, M. The feasibility of solar-powered small-scale brackish water desalination units in a coastal aquifer prone to saltwater intrusion: A comparison between electro dialysis reversal and reverse osmosis. *J. Environ. Manag.* **2021**, *290*, 112604. [[CrossRef](#)]
8. Liu, B.X.; Wang, S.Q.; Kong, X.L.; Liu, X.J.; Sun, H.Y. Modeling and assessing feasibility of long-term brackish water irrigation in vertically homogeneous and heterogeneous cultivated lowland in the North China Plain. *Agric. Water Manag.* **2019**, *211*, 98–110. [[CrossRef](#)]
9. Nicolas, E.; Alarcon, J.J.; Mounzer, O.; Pedrero, F.; Nortes, P.A.; Alcobendas, R.; Romero-Trigueros, C.; Bayona, J.M.; Maestre-Valero, J.F. Long-Term Physiological and Agronomic Responses of Mandarin Trees to Irrigation with Saline Reclaimed Water. *Agric. Water Manag.* **2016**, *166*, 1–8. [[CrossRef](#)]
10. Gebrehiwet, M.; Tafesse, N.T.; Habtu, S.; Alemaw, B.F.; Laletsang, K.; Lasarwe, R. The contribution of groundwater to the salinization of reservoir-based irrigation systems. *Agronomy* **2021**, *11*, 512. [[CrossRef](#)]
11. Zhang, L.; Chen, S.; Wu, L.; Huang, J.; Tian, C.; Zhang, J.; Cao, X.; Zhu, C.; Kong, Y.; Jin, Q.; et al. Effects of Nitrogen Fertilizer Reduction and Oxygen-Enhancing Irrigation on the Key Enzyme Activities of Nitrogen Metabolism and Nitrogen Utilization in Rice. *Trans. Chin. Soc. Agric. Eng.* **2022**, *38*, 81–90.
12. Baram, S.; Weinstein, M.; Evans, J.F.; Berezkin, A.; Sade, Y.; Ben-Hur, M.; Bernstein, N.; Mamane, H. Drip irrigation with nanobubble oxygenated treated wastewater improves soil aeration. *Sci. Hortic.* **2022**, *291*, 110550. [[CrossRef](#)]
13. Lu, J.; Li, X.N.; Yang, Y.L.; Jia, L.Y.; You, J.; Wang, W.R. Effect of hydrogen peroxide on seedling growth and antioxidants in two wheat cultivars. *Biol. Plant.* **2013**, *57*, 487–494. [[CrossRef](#)]
14. Abd Elhady, S.A.; El-Gawad, H.G.; Ibrahim, M.F.M.; Mukherjee, S.; Elkelish, A.; Azab, E.; Gobouri, A.A.; Farag, R.; Ibrahim, H.A.; El-Azm, N.A. Hydrogen peroxide supplementation in irrigation water alleviates drought stress and boosts growth and productivity of potato plants. *Sustainability* **2021**, *13*, 899. [[CrossRef](#)]
15. Ahmed, A.K.A.; Shi, X.N.; Hua, L.K.; Manzueta, L.; Qing, W.H.; Marhaba, T.; Zhang, W. Influences of air, oxygen, nitrogen, and carbon dioxide nanobubbles on seed germination and plant growth. *J. Agric. Food Chem.* **2018**, *66*, 5117–5124. [[CrossRef](#)]
16. Zhang, Z.P.; Ju, Z.L.; Wells, M.C.; Walter, R.B. Genomic approaches in the identification of hypoxia biomarkers in model fish species. *J. Exp. Mar. Bio. Ecol.* **2009**, *381*, S180–S187. [[CrossRef](#)]
17. Zhang, K.; Tian, C.Y.; Li, C.J. Root growth and spatio-temporal distribution of three common annual halophytes in a saline desert, northern Xinjiang. *J. Arid. Land.* **2012**, *4*, 330–341. [[CrossRef](#)]
18. de Bang, T.C.; Lay, K.S.; Scheible, W.R.; Takahashi, H. Small peptide signaling pathways modulating macronutrient utilization in plants. *Curr. Opin. Plant Biol.* **2017**, *39*, 31–39. [[CrossRef](#)]
19. Wang, R.; Shi, W.M.; Li, Y.L. Link between aeration in the rhizosphere and P-acquisition strategies: Constructing efficient vegetable root morphology. *Front. Environ. Sci.* **2020**, *10*, 906893. [[CrossRef](#)]
20. Zan, O.Y.; Tian, J.C.; Yan, X.F.; Shen, H. Effects of different concentrations of dissolved oxygen or temperatures on the growth, photosynthesis, yield and quality of lettuce. *Agric. Water Manag.* **2019**, *228*, 105896.
21. Lopez-Pozos, R.; Martinez-Gutierrez, G.A.; Perez-Pacheco, R.; Urrestarazu, M. The effects of slope and channel nutrient solution gap number on the yield of tomato crops by a nutrient film technique system under a warm climate. *Hortscience* **2011**, *46*, 727–729. [[CrossRef](#)]
22. Xu, C.M.; Chen, L.P.; Chen, S.; Chu, G.; Wang, D.Y.; Zhang, X.F. Effects of rhizosphere oxygen concentration on root physiological characteristics and anatomical structure at the tillering stage of rice. *Ann. Appl. Biol.* **2020**, *177*, 61–73. [[CrossRef](#)]
23. McMinn, A.; Pankowski, A.; Delfatti, T. Effect of hyperoxia on the growth and photosynthesis of polar sea ice microalgae. *J. Phycol.* **2005**, *41*, 732–741. [[CrossRef](#)]
24. Huang, J.X.; Gomez-Dans, J.L.; Huang, H.; Ma, H.Y.; Wu, Q.L.; Lewis, P.E.; Liang, S.L.; Chen, Z.X.; Xue, J.H.; Wu, Y.T.; et al. Assimilation of remote sensing into crop growth models: Current status and perspectives. *Agric. For. Meteorol.* **2019**, *276*, 107609. [[CrossRef](#)]
25. Shi, P.J.; Ishikawa, T.; Sandhu, H.S.; Hui, C.; Chakraborty, A.; Jin, X.S.; Tachihara, K.; Li, B.L. On the 3/4-exponent von Bertalanffy equation for ontogenetic growth. *Ecol. Model.* **2014**, *276*, 23–28. [[CrossRef](#)]
26. Liu, F.L.; Liu, Y.H.; Su, L.J.; Tao, W.H.; Wang, Q.J.; Deng, M.J. Integrated Growth Model of Typical Crops in China with Regional Parameters. *Water* **2022**, *14*, 1139. [[CrossRef](#)]
27. Yin, X.Y.; Goudriaan, J.; Lantinga, E.A.; Vos, J.; Spiertz, H.J. A flexible sigmoid function of determinate growth. *Ann. Bot.* **2003**, *91*, 361–371. [[CrossRef](#)]
28. Zou, Y.F.; Saddique, Q.; Dong, W.J.; Zhao, Y.; Zhang, X.; Liu, J.C.; Ding, D.Y.; Feng, H.; Wendroth, O.; Siddique, K.H.M. Quantifying the compensatory effect of increased soil temperature under plastic film mulching on crop growing degree days in a wheat–maize rotation system. *Field Crop. Res.* **2021**, *260*, 107993. [[CrossRef](#)]

29. Hocaoglu, O.; Gonulal, E.; Akcura, M. Modelling the effect of irrigation deficit on maize growth with Logistic regression. *Commun. Soil Sci. Plan.* **2023**, *54*, 1293–1305. [[CrossRef](#)]
30. Herrera, J.M.; Stamp, P.; Liedgens, M. Interannual variability in root growth of spring wheat (*Triticum aestivum* L.) at low and high nitrogen supply. *Eur. J. Agron.* **2007**, *26*, 317–326. [[CrossRef](#)]
31. Hammad, H.M.; Abbas, F.; Ahmad, A.; Bakhat, H.F.; Farhad, W.; Wilkerson, C.J.; Fahad, S.; Hoogenboom, G. Predicting kernel growth of maize under controlled water and nitrogen applications. *Int. J. Plant Prod.* **2020**, *14*, 609–620. [[CrossRef](#)]
32. Yu, Q.; Liu, J.D.; Zhang, Y.Q.; Li, J. Simulation of rice biomass accumulation by an extended logistic model including influence of meteorological factors. *Int. J. Biometeorol.* **2002**, *46*, 185–191. [[CrossRef](#)] [[PubMed](#)]
33. Shabani, A.; Sepaskhah, A.R.; Kamgar-Haghighi, A.A. Estimation of yield and dry matter of rapeseed using Logistic model under water salinity and deficit irrigation. *Arch. Agron. Soil Sci.* **2014**, *60*, 951–969. [[CrossRef](#)]
34. Wang, K.; Su, L.J.; Wang, Q.J. Cotton growth model under drip irrigation with film mulching: A case study of Xinjiang, China. *Agron. J.* **2021**, *113*, 2417–2436. [[CrossRef](#)]
35. Zhu, Z.C.; Friedman, S.P.; Chen, Z.J.; Zheng, J.N.; Sun, S.J. Dry matter accumulation in maize in response to film mulching and plant density in northeast China. *Plants* **2022**, *11*, 1411. [[CrossRef](#)] [[PubMed](#)]
36. Zhu, H.F.; Li, X.F.; Khalid, M.; Xi, D.D.; Zhang, Z.H.; Zhu, Y.Y. Growth and physiological responses of selected pakchoi varieties to *Plasmodiophora brassicae* infection. *J. Plant Pathol.* **2020**, *102*, 459–467. [[CrossRef](#)]
37. Jeon, J.; Lim, C.J.; Kim, J.K.; Park, S.U. Comparative metabolic profiling of green and purple pakchoi (*Brassica Rapa* Subsp. *Chinensis*). *Molecules* **2018**, *23*, 1613. [[CrossRef](#)]
38. Ding, D.Y.; Feng, H.; Zhao, Y.; Hill, R.L.; Yan, H.M.; Chen, H.X.; Hou, H.J.; Chu, X.S.; Liu, J.C.; Wang, N.J.; et al. Effects of continuous plastic mulching on crop growth in a winter wheat-summer maize rotation system on the Loess Plateau of China. *Agric. For. Meteorol.* **2019**, *271*, 385–397. [[CrossRef](#)]
39. Gu, S. Growing degree hours—a simple, accurate, and precise protocol to approximate growing heat summation for grapevines. *Int. J. Biometeorol.* **2016**, *60*, 1123–1134. [[CrossRef](#)]
40. Sun, Y.; Wang, Y.C.; Wang, Q.J. Effects of oxygenated brackish water on light response characteristics and yield of pakchoi (*Brassica chinensis* L.). *Trans. Chin. Soc. Agric. Eng.* **2020**, *36*, 116–123. (In Chinese)
41. Zhu, M.J.; Wang, Q.J.; Sun, Y.; Zhang, J.H. Effects of oxygenated brackish water on germination and growth characteristics of wheat. *Agric. Water Manag.* **2021**, *245*, 106520. [[CrossRef](#)]
42. Licausi, F. Molecular elements of low-oxygen signaling in plants. *Physiol. Plant.* **2013**, *148*, 1–8. [[CrossRef](#)] [[PubMed](#)]
43. Zhang, M.; Smith, J.A.C.; Harberd, N.P.; Jiang, C.F. The regulatory roles of ethylene and reactive oxygen species (ROS) in plant salt stress responses. *Plant Mol. Biol.* **2016**, *91*, 651–659. [[CrossRef](#)] [[PubMed](#)]
44. Sultana, M.S.; Yamamoto, S.I.; Biswas, M.S.; Sakurai, C.; Isoai, H.; Mano, J. Histidine-containing dipeptides mitigate salt stress in plants by scavenging reactive carbonyl species. *J. Agric. Food Chem.* **2022**, *70*, 11169–11178. [[CrossRef](#)]
45. Gill, S.S.; Tuteja, N. Reactive oxygen species and antioxidant machinery in abiotic stress tolerance in crop plants. *Plant Physiol. Biochem.* **2010**, *48*, 909–930. [[CrossRef](#)]
46. Chatterjee, A.; Singh, S.; Rai, R.C.; Rai, S.; Rai, L.C. Functional characterization of Alr0765, a hypothetical protein from anabaena PCC 7120 involved in cellular energy status sensing, iron acquisition and abiotic stress management in *E. coli* using molecular, bio-chemical and computational approaches. *Curr. Genom.* **2020**, *21*, 295–310. [[CrossRef](#)]
47. Fan, W.; Zhou, Z.; Wang, W.T.; Huo, M.X.; Zhang, L.L.; Zhu, S.Y.; Yang, W.; Wang, X.Z. Environmentally friendly approach for advanced treatment of municipal secondary effluent by integration of micro-nano bubbles and photocatalysis. *J. Clean. Prod.* **2019**, *237*, 117828. [[CrossRef](#)]
48. Wang, Z.; Yi, K.Y.; Lin, Q.Y.; Yang, L.; Chen, X.S.; Chen, H.; Liu, Y.Q.; Wei, D.C. Free radical sensors based on inner-cutting graphene field-effect transistors. *Nat. Commun.* **2019**, *10*, 1544. [[CrossRef](#)]
49. Smirnoff, N.; Arnaud, D. Hydrogen peroxide metabolism and functions in plants. *New Phytol.* **2019**, *221*, 1197–1214. [[CrossRef](#)]
50. Li, P.; Takahashi, M.; Chiba, K. Enhanced free-radical generation by shrinking microbubbles using a copper catalyst. *Chemosphere* **2009**, *77*, 1157–1160. [[CrossRef](#)]
51. Lemke, M.D.; Woodson, J.D. Targeted for destruction: Degradation of singlet oxygen-damaged chloroplasts. *Plant Signal. Behav.* **2022**, *17*, 2084955. [[CrossRef](#)] [[PubMed](#)]
52. Novriyanti, E.; Watanabe, M.; Makoto, K.; Takeda, T.; Hashidoko, Y.; Koike, T. Photosynthetic nitrogen- and water-use efficiency of acacia and eucalypt seedlings as afforestation species. *Photosynthetica* **2012**, *50*, 273–281. [[CrossRef](#)]
53. Sever, K.; Bogdan, S.; Skvorc, Z. Response of photosynthesis, growth, and acorn mass of pedunculate oak to different levels of nitrogen in wet and dry growing seasons. *J. For. Res.* **2023**, *34*, 167–176. [[CrossRef](#)]
54. Zhang, Z.H.; Cao, B.L.; Chen, Z.J.; Xu, K. Grafting enhances the photosynthesis and nitrogen absorption of tomato plants under low-nitrogen stress. *J. Plant Growth Regul.* **2022**, *41*, 1714–1725. [[CrossRef](#)]

55. Pendergast, L.; Bhattarai, S.P.; Midmore, D.J. Benefits of oxygation of subsurface drip-irrigation water for cotton in a Vertosol. *Crop Pasture Sci.* **2013**, *64*, 1171–1181. [[CrossRef](#)]
56. Tilly, N.; Aasen, H.; Bareth, G. Fusion of plant height and vegetation indices for the estimation of barley biomass. *Remote Sens.* **2015**, *7*, 11449–11480. [[CrossRef](#)]

Disclaimer/Publisher’s Note: The statements, opinions and data contained in all publications are solely those of the individual author(s) and contributor(s) and not of MDPI and/or the editor(s). MDPI and/or the editor(s) disclaim responsibility for any injury to people or property resulting from any ideas, methods, instructions or products referred to in the content.